An Investigation of Motorcycle Stability and Control

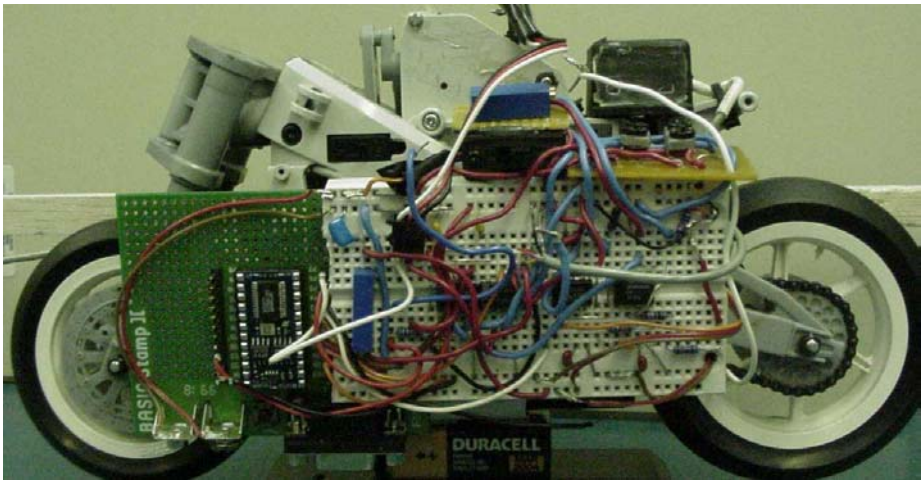

Thomas Douglas Hull

May 18, 2000

INTRODUCTION

It is well known that the motorcycle rider acts both a structural property as well as a controller for the unstable motorcycle system. Using equations of motion for steady state motorcycle running developed by R. Sharp in 1971, computer simulations will be compared to experimental results obtained by using a scale motorcycle on a conveyor testbed.

MOTORCYCLE MODEL

The basic model uses the linearized equations from Sharp's 4 degree of freedom system. The four degrees of freedom are yaw angle, ψ, roll angle, ϕ, lateral cycle position, y, and steering angle, δ as shown below. Since we are concerned with steady state running conditions, the longitudinal velocity, V_x, is fixed. The motorcycle itself is modeled as a front and rear mass (M_f , M_r) hinged together at the front fork as shown below in Fig. A and Fig. B.

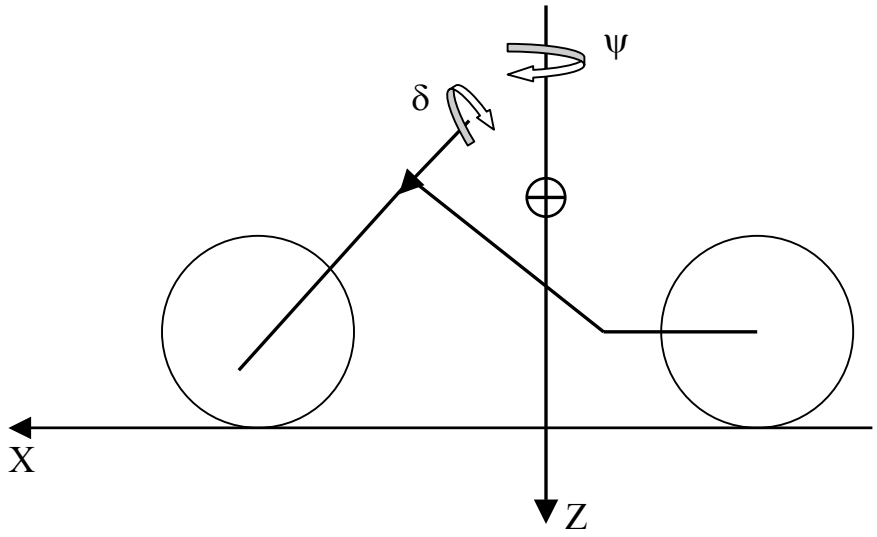

Fig. A. Motorcycle Model Side View.

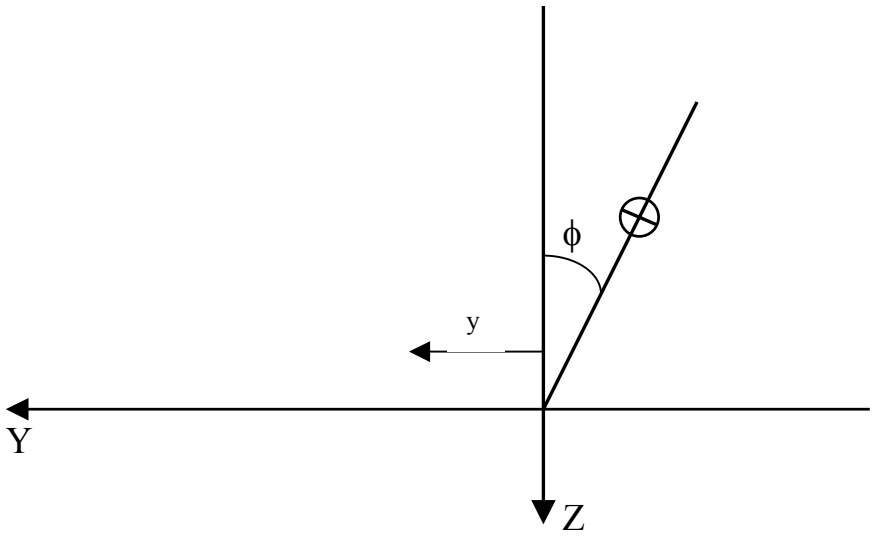

Fig. B. Motorcycle/Rider Model Rear View.

Equations of motion were derived by Sharp using the Lagrangian method. The full model consists of ten differential equations, four for that of the cycle, two representing the front/rear lateral tire forces (Y_f , Y_r), two representing the front/rear aligning moments (T_{zf} , T_{zr}), and two representing the front/rear overturning moments (T_{xf} , T_{xr}). The last six equations use tire data based on tire relaxation lengths (and tire normal force). The tires are modeled as a first-order lag system. All twelve equations of motion were taken Sharp [4] and Katayama [1]. The equations of motion are:

$$(M_{f0} + M_r)(\ddot{y} + V\dot{\psi}) + M_f k\ddot{\psi} + (M_f j + M_r h)\ddot{\phi} + M_f e\ddot{\delta} - Y_f - Y_r = 0 \tag{1}$$

$$M_f k\ddot{y} + (M_f ek + I_{fz}\cos\varepsilon)\ddot{\delta} - \frac{i_{fy}}{R_f}\sin\varepsilon\ V\dot{\delta} + \{M_f jk - C_{rxz} + (I_{fz} - I_{fx})\sin\varepsilon\cos\varepsilon\}\ddot{\phi}$$
$$-\left(\frac{i_{fy}}{R_f} + \frac{i_{ry} + \lambda i}{R_r}\right)V\dot{\varphi} + (M_f k^2 + I_{rz} + I_{fx}\sin^2\varepsilon + I_{fz}\cos^2\varepsilon)\ddot{\psi} + M_f kV\dot{\psi} - l_1 Y_f + l_2 Y_r - T_{zf} - T_{zr} = -\tau\cos\varepsilon \tag{2}$$

$$\left(M_f j + M_r h\right)\ddot{y} + \left(M_f e j + I_{fz}\sin\varepsilon\right)\ddot{\delta} + \frac{i_{fy}}{R_f}\cos\varepsilon\, V\dot{\delta} + \left(t Z_f - M_f e g\right)\delta + \left(M_f j^2 + M_r h^2 + I_{rx} + I_{fx}\cos^2\varepsilon + I_{fz}\sin^2\varepsilon\right)\ddot{\phi}$$

$$- \left(M_f j + M_r h\right) g\phi + \left\{M_f jk - C_{rxz} + \left(I_{fz} - I_{fx}\right)\sin\varepsilon\cos\varepsilon\right\}\ddot{\psi} + \left(M_f j + M_r h + \frac{i_{fy}}{R_f} + \frac{i_{ry} + \lambda i}{R_r}\right) V\dot{\psi} - T_{xf} - T_{xr} = 0 \quad (3)$$

$$M_f e\ddot{y} + \left(I_{fz} + M_f e^2\right)\ddot{\delta} + K\dot{\delta} + \left(t Z_f - M_f e g\right)\sin\varepsilon\,\delta + \left(M_f e j + I_{fz}\sin\varepsilon\right)\ddot{\phi} - \frac{i_{fy}}{R_f}\cos\varepsilon\, V\dot{\phi} + \left(t Z_f - M_f e g\right)\phi$$

$$+ \left(M_f e k + I_{fz}\cos\varepsilon\right)\ddot{\psi} + \left(M_f e + \frac{i_{fy}}{R_f}\sin\varepsilon\right) V\dot{\psi} + t Y_f - T_{zf}\cos\varepsilon - T_{xf}\sin\varepsilon = \tau \quad (4)$$

$$\frac{\sigma_f}{V}\dot{Y}_f + Y_f - C_{f1}\left(\delta\cos\varepsilon - \frac{\dot{y} + l\dot{\psi} - t\dot{\delta}}{V}\right) - C_{f2}\left(\phi + \delta\sin\varepsilon\right) = 0 \quad (5)$$

$$\frac{\sigma_r}{V}\dot{Y}_r + Y_r - C_{r1}\left(\frac{b\dot{\psi} - \dot{y}}{V}\right) - C_{r2}\phi = 0 \quad (6)$$

$$\frac{\sigma_f}{V}\dot{T}_{zf} + T_{zf} - VC_{zs1}\dot{y} - Vl_1 C_{zs1}\dot{\psi} + VtC_{zs1}\delta - C_{zc1}\phi + \left(C_{zs1}\cos\varepsilon - C_{zc1}\sin\varepsilon\right)\delta = 0 \quad (7)$$

$$\frac{\sigma_r}{V}\dot{T}_{zr} + T_{zr} - VC_{zs2}\dot{y} + Vl_2 C_{zs2}\dot{\psi} - C_{zs2}\phi = 0 \quad (8)$$

$$\frac{\sigma_f}{V}\dot{T}_{xf} + T_{xf} - VC_{xs1}\dot{y} - Vl_1 C_{xs1}\dot{\psi} + C_{xs1}tV\dot{\delta} + C_{xc1}\phi + \left(C_{xs1}\cos\varepsilon - C_{xc1}\sin\varepsilon\right)\delta = 0 \quad (9)$$

$$\frac{\sigma_r}{V}\dot{T}_{xr} + T_{xr} - VC_{xs2}\dot{y} + Vl_2 C_{xs2}\dot{\psi} + C_{xs2}\phi = 0 \quad (10)$$

where the model parameters are taken from [1], except the tire data, which was taken from Katayama [2] due to several errors in [1]. The motorcycle/rider data was taken from the Japan Automobile Research Institute and can be found in Appendix A. The data is that of a medium sized sport motorcycle with an "average" sized rider.

To set up the simulations, the equations of motion were converted to a block diagram form using SIMULINK as shown in Fig. 1. The entire system consists of 14 integrators

and 4 differentiators. Time stepping was set to auto and no convergence problems were observed throughout the simulations. Typical time steps of 1 ms were observed.

SCALE MODEL

To facilitate experiments, a scale motorcycle was constructed using a 1/8 scale Kyosho® RC motorcycle chassis. The cycle was originally steered using a cambering front wheel mechanism. The cambering mechanism was disabled and the front fork was "locked" to a zero degree position so that a steering torque along the steering fork axis was the only method for steering the motorcycle. To replicate the actions of a rider, a steering linkage was constructed to apply a steering torque using a standard high speed Futaba servo. The linkage, shown schematically in Fig. C uses a servo displacement to generate a torque. Two equal stiffness (k) springs are in compression, sandwiching the servo arm. The compression force is adjustable by moving the wheel collars. The steering balljoint allows for minimal friction along the steer axis and avoids binding at the servo horn/pushrod connection.

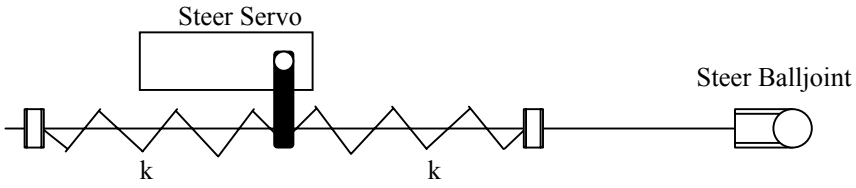

Fig. C. Steering Torque Mechanism.

The scale motorcycle was also equipped with a Crossbow CXTA01 analog tilt sensor. The sensor data sheet can be found in Appendix B. The motorcycle speed was controlled using the standard on-board electronic speed control operated by the user, while the

steering servo was commanded using an on board microprocessor, the STAMP BS2-Sx (see data sheet in Appendix B). The analog tilt sensor output is read into the microprocessor input by way of the Analog Devices ADC 0831 analog to digital converter. Control algorithms were coded using a PBASIC compiler and downloaded to the on-board controller using a serial connection in a standard DOS environment on a personal computer. Once a program was downloaded, the scale motorcycle was autonomous except for longitudinal speed control, which was controlled using the RC controller to match the conveyor speed. Additional hardware including an IR distance measuring sensor was added for use in trajectory tracking (lane changes). The Sharp GP2D12 analog IR sensor (see data sheet in Appendix B) was mounted on a balsa wood beam approximately 12 inches in front of the motorcycle to measure lateral distance from a fixed object. The signal was low pass filtered to avoid any RF noise interference and then sent to the STAMP using the Analog Devices ADC 0831 analog to digital converter. The microcontroller could output a pulse width modulated signal to the steering servo. Varying the length of the signal high between 1 and 2 ms at a period of at least every 20 ms commanded the servo to positions of about +-20 degrees from the neutral position (zero torque). Other inputs to the microcontroller included a calibration switch, which would indicate when the processor should store calibration points and begin closed loop control. The scale motorcycle is shown in Fig. D and Fig. E on the following page.

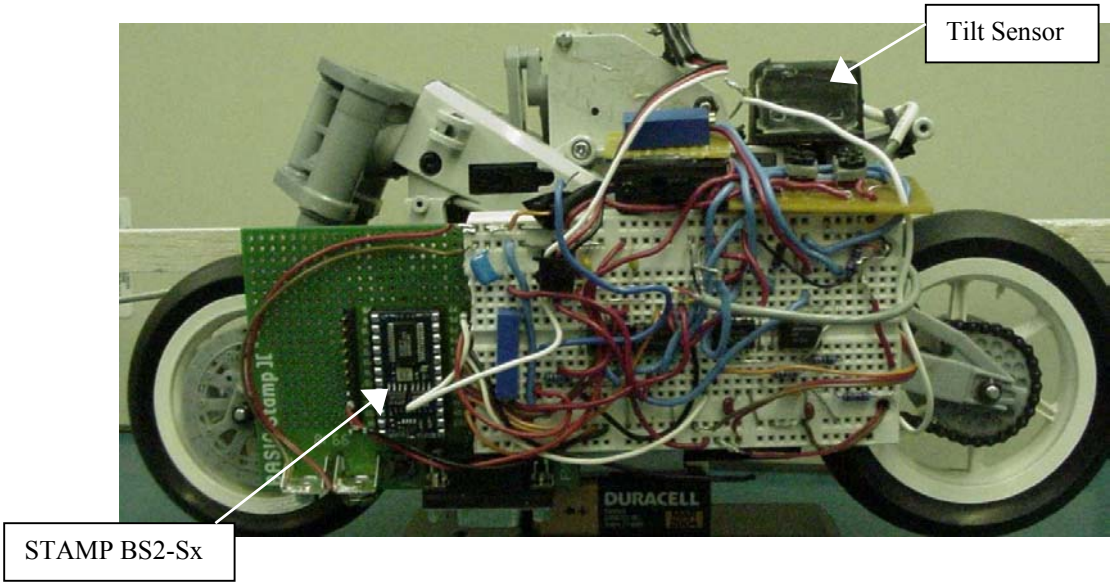

Fig D. Scale Motorcycle LHS.

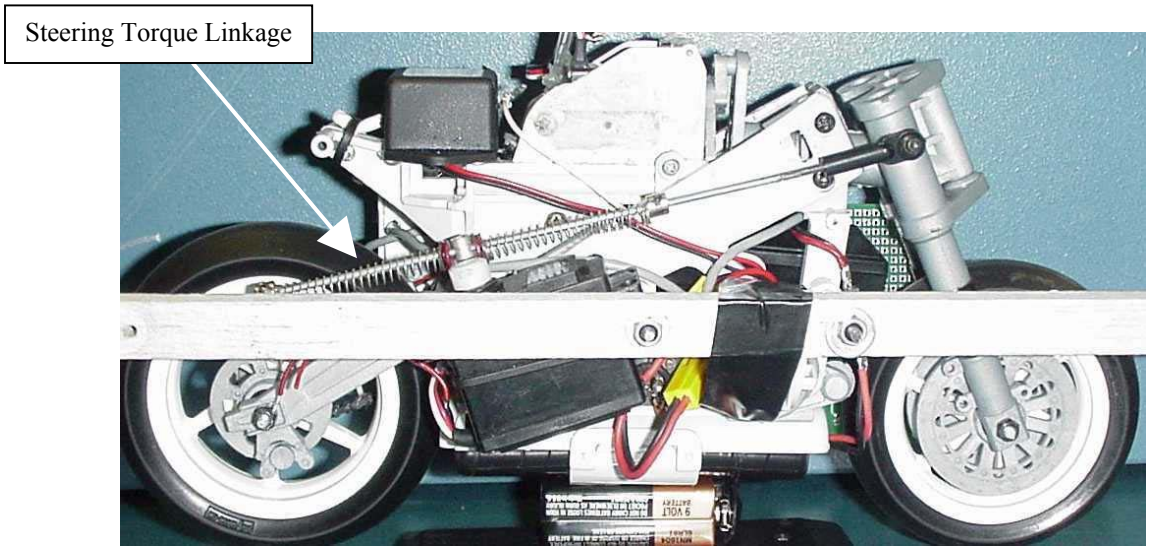

Fig. E. Scale Motorcycle RHS.

STABILITY ANALYSIS

To investigate motorcycle stability, the ten linear differential equations of motion were reduced to a set of 12 first order equations as shown in Appendix C. By assembling the first order equations in state-space form:

$$\dot{z} = [A]z,$$

system stability can be examined by investigating the eigenvalues of the [A] matrix. Matlab was used to numerically find the eigenvalues of the 10 by 10 matrix as shown in Appendix A. First, free control motorcycle stability was investigated. In free control, the steering axis degree of freedom, δ, is included in the equations of motion. The free control eigenvalues versus motorcycle longitudinal velocity are plotted in Fig. 2. The plot shows there are three modes of motorcycle instability. The first mode is referred to as the weave mode, and is unstable up to about 10 m/s. Once stable, the weave mode remains stable throughout the speed range of interest. The weave mode has been observed experimentally and is an combined roll/yaw oscillation. The capsize mode of the motorcycle should NOT be interpreted too literally. The plot shows the capsize mode eigenvalues to be stable at low speeds and approaching the imaginary axis at very high speeds. When the capsize mode becomes unstable, the motorcycle is no longer a counter-steered vehicle. Finally, the wobble mode is stable at low speeds and becomes unstable at about 43 m/s. The wobble mode is a steering oscillation much like the wheel shimmy present in some light aircraft nosewheels. Experiments using the scale model verified the presence of the weave mode. At very low speeds, the motorcycle will fall over. At conveyor speeds above approximately 2 m/s, the motorcycle is self-stabilizing, much like

the hands-off control of a bicycle. Wobble and capsize instability modes were not observed in experiments, probably due to the lower conveyor speeds (below 3.5 m/s).

It was observed in experiments that the scale motorcycle is not controllable using rigid displacement steering control instead of steering torque control. The motorcycle was unstable at ALL speeds. A numerical stability analysis was conducted omitting the steering degree of freedom. The resultant fixed control equations of motion are shown in Appendix C. The nine equations of motion were reduced to 10 first order equations, and eigenvalues of the system versus longitudinal velocity were plotted in Fig. 3. The plot clearly shows the motorcycle is unstable at all speeds with the weave mode unstable over the entire speed range, which agrees with experiments. This verifies that a motorcycle depends on free control of the steering axis for stability. These findings motivated the design of a mechanism which would generate a steer torque while still allowing free control of the steer axis. The design is shown pictorially in Fig. F.

Fig. F. Steering Torque Mechanism Top View.

Finally, the effects of proportional plus derivative control on the roll angle feedback with free control were examined. The steering torque input, τ, was then considered with:

$$\tau = K_p(\phi) + K_d(\dot{\phi}),$$

Where ϕ is the roll angle and ϕ dot is the time derivative of the roll angle. The eigenvalues versus motorcycle longitudinal velocity are shown in Fig. 4. The modes of instability follow the same behavior of the open loop free control, except the weave mode is shifted to the left. The left shift shows that proportional derivative control (K_p= 10, K_p= 200) will stabilize the motorcycle at a lower motorcycle longitudinal velocity, in this case the motorcycle becomes open loop stable at just above 7 m/s compared with the open loop free control value of just under 10 m/s. This agrees with the fact that a rider can stabilize a motorcycle at lower speeds as compared to a riderless motorcycle.

SIMULATION RESULTS

Using a model created with Matlab SIMULINK, motorcycle responses to non-zero roll initial conditions and lane change maneuvers were simulated. The model parameters can be found in Appendix A. First a simple proportional control was used on the roll angle feedback. The roll angle response to a 10 degree initial condition is shown in Fig. 5. The response is oscillatory as one would expect because we are not using pole placement to stabilize the motorcycle. The response shows simple proportional control is not enough to stabilize the motorcycle at a zero degree roll condition. Using proportional plus derivative control on roll angle feedback (using a SIMULINK continuous differentiator) as shown in Fig. G can stabilize the roll angle above a critical speed.

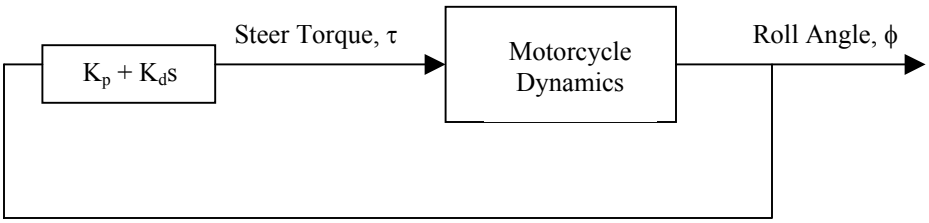

Fig. G. Feedback Control Loop for Roll Stabilization.

The roll angle response using PD control to a 10 degree initial condition and longitudinal velocity of 60 km/hr is shown in Fig. 6. The roll angle settles to zero degrees in a critically damped fashion. The steering torque for the maneuver is shown in Fig. 7. The steering torque is oscillatory, and probably due to the sensitive derivative term. The gains used for this simulation are K_p= 156, K_d= 50. Proportional derivative control can only stabilize the motorcycle above a critical speed, under which the motorcycle is unstable. A longitudinal velocity of 8 km/hr is the onset of instability as shown in Fig. 8. At this velocity, the roll angle response becomes oscillatory, similar to the behavior of proportional control alone at a longitudinal velocity of 60 km/hr. At a longitudinal velocity of 5 km/hr, the system is unstable as shown in Fig. 9. The roll angle response is an increasing amplitude oscillation. These results agree with the aforementioned stability analysis; pole placement will shift the weave mode curve to the left, making the motorcycle stable at a lower speed or effectively lowering the critical speed of the weave mode.

Lane change maneuvers were then simulated using the same model with the simplified control:

$$\tau = Ks_{\phi} * \phi + Ks_d * d \,, \qquad \text{(Steer Torque)}$$

and

$$d = (y_{desired} - y_{actual}) + L_{prev} * (\Psi_{desired} - \Psi_{actual}), \qquad \text{(lateral error)}$$

where y is the lateral position, L_{prev} is the preview distance, and $\Psi_{desired}$ is the desired yaw angle, zero. With Ks_{ϕ}=156, Ks_{d}=-5.6 (countersteer), Fig. 10 shows a lane change lateral position response and its corresponding trajectory with a lateral displacement of 2 meters. The response shows some overshoot, which is mainly a result of the simplified lateral distance calculation versus a comprehensive lateral heading error calculation (basically an integration of forward heading errors). The response is satisfactory in the fact the motorcycle follows the prescribed trajectory. The roll angle response is shown in Fig. 11. The roll angle reaches a maximum of just under 3 degrees. The yaw angle response to the lane change maneuver is plotted in Fig 12. The maximum yaw angle achieved is less than 2 degrees and occurs just before the motorcycle overshoots its intended trajectory. The yaw angle is very small, implying the motorcycle relies HEAVILY on lateral tire forces generated from wheel camber instead of large steering and hence large yaw angles as would be the case for automobiles. Finally, a lane change maneuver was simulated using a preview distance of zero, basically simplifying the steering torque control to:

$$\tau = Ks_{\phi} * \phi + Ks_{d} * (y_{desired} - y_{actual}),$$

which makes the controller non-anticipative, similar to trying to follow a prescribed trajectory while looking directly downward at it. The lateral position response is shown in Fig. 13. The result is what one would expect; the response is oscillatory unstable, and the motorcycle cannot track the trajectory. The roll angle response is also unstable with a growing oscillatory behavior as shown in Fig. 14.

Experiments

Experiments were conducted using the scale motorcyle on the conveyor testbed. First, code was written to implement proportional derivative control on the roll angle feedback to stabilize the weave mode of instability at lower motorcycle speeds. The code was written in PBASIC and is shown in Appendix D. The control algorithm works as follows: the motorcycle is first run on the conveyor in open loop until the system stabilizes to a constant roll angle. Once at a near zero equilibrium roll angle, the user then sets a normally high input pin to low. At this point, the STAMP will store the calibrated roll angle and use it as the reference angle in the control loop. The STAMP will then go into closed loop mode with PD control on the roll angle feedback. The incoming roll angle signal is first low pass filtered using a second order butterworth filter followed by a digital filter which uses the average of the past three samples to avoid unwanted noise. The steering torque will then be generated by the steer servo, which is commanded by the STAMP pulse width signal as discussed previously.

The scale motorcycle is open loop stable above longitudinal velocities of 2 m/s. Using proportional derivative control on the roll angle feedback, the motorcycle is self-stabilizing to just above 1 m/s. That speed is highly dependent upon the gains used at the controller as well as motorcycle balance and the compression of the steering torque springs (also the spring stiffness). A plot of the servo voltage and roll angle response is shown if Fig. 15. The experimental results of this plot are very difficult to decipher, and do not adequately describe what is going on. The bike was stabilized (but still wandered on the conveyor). The roll angle response voltage shows the bike did stay at a constant roll voltage (hence angle). The servo voltage response does show the servo moved

during the experiment, but it is difficult to tell how the roll angle responded. This is because the servo voltage and roll angle voltages changed very little throughout the experiment as the motorcycle was near equilibrium and only small perturbations from the calibrated roll angle were allowed before control action was taken. The plot also contains a lot of RF noise, which was a consequence of having long wires (which were shielded) for data acquisition.

Trajectory tracking was tried in experiments unsuccessfully. The bike was equipped with an IR distance sensor mounted about L=12 inches in front of the bike on a balsa wood boom. The boom was used to anticipate lane change lateral errors as shown in Fig H and pictorially in Fig. I.

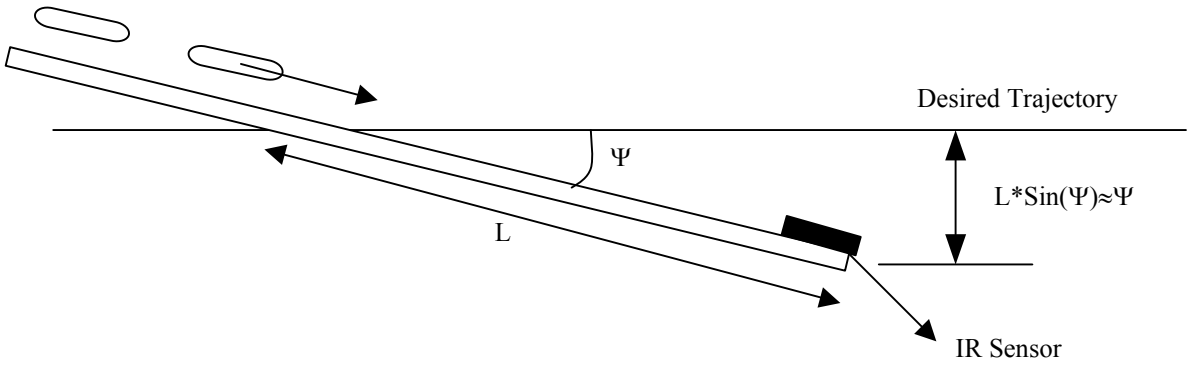

Fig. H. Lateral Heading Error Using IR Sensor Mounted on Boom.

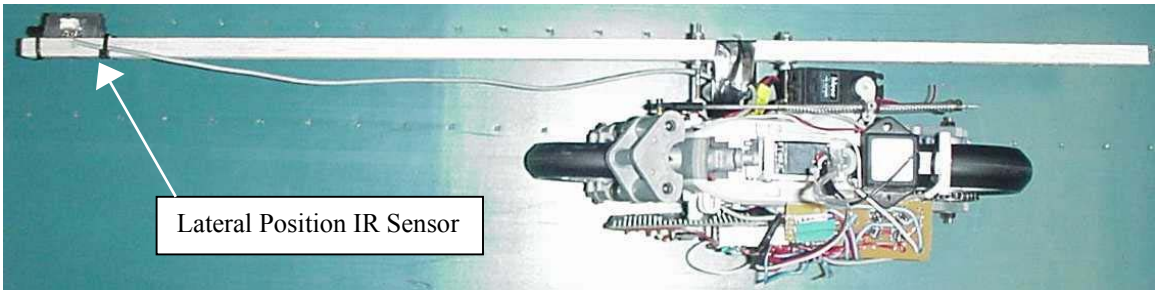

Fig. I. Lateral Position Sensor Apparatus.

The trajectory tracking controller used roll angle feedback as before, but now the reference signal came from the master/slave control system shown in Fig. J.

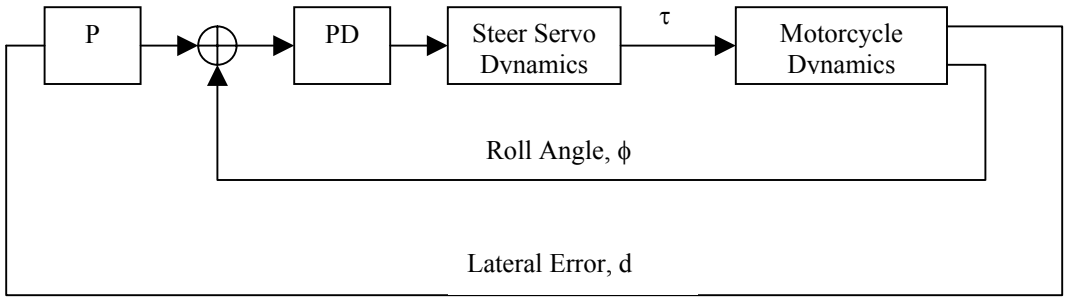

Fig. J. Master/Slave Control for Trajectory Tracking.

The code for this controller is in Appendix D. Experiments showed the motorcycle cannot follow a trajectory using the lateral error calculation (sensor mounted on a boom) because the motorcycle does not yaw appreciably, and hence the controller cannot be anticipative. Instead, the response is an oscillation of growing amplitude just as the simulation with zero preview distance shows in Fig. 13. Experimental data was collected for the unstable response, and is shown in Fig. 16 and Fig. 17. The responses contain too much RF noise to decipher what is really happening, despite the addition of data acquisition wire shielding and an RF choke. The author did observe the same qualitative behavior as the zero preview distance simulation. Furthermore, it was easy to see the motorcycle DOES NOT yaw appreciably, especially when compared to the yaw angles of a scale motor vehicle.

CONCLUSIONS

This investigation showed there are three modes of motorcycle instability, namely the weave, wobble, and capsize. Stabilization of the weave mode was accomplished in experiments using proportional derivative control on the steering torque input. The proportional derivative control will shift the weave mode eigenvalues leftwards, so that the motorcycle system will be stable at a lower critical speed. This is well observed in experiments, as a rider can stabilize the motorcycle at speeds that the open loop motorcycle system is unstable. Motorcycles rely heavily on wheel cambering to produce lateral tire forces. Trajectory tracking is not possible (at least not with the hardware accuracy used in experiments) using a lateral error based on yaw angle because typical motorcycle yaw angles during a lane change maneuver are very small, on the order of a just a few degrees. Attempting to track a trajectory using such a lateral error calculation based on yaw angles will cause the motorcycle to be oscillatory unstable with growing amplitude oscillations.

REFERENCES

1. Katayama, T., Aoki, A., Nishimi, T., Control Behaviour of Motorcycle Riders, Vehicle System Dynamics, 17 (1988), pp. 211-229.
2. Katayama, T., Nishimi, T., Energy Flow Method for Study of Motorcycle Wobble Mode, Vehicle System Dynamics, 19 (1990), pp. 151-175.
3. Sharp, R.S., The Lateral Dynamics of Motorcycles and Bicycles, Vehicle System Dynamics, 14 (1985), pp. 265-283.
4. Sharp, R.S. The Stability and Control of Motorcycles. Journal of Mechanical Engineering Science, 13 (1972), pp. 316-328.

Appendix A: Matlab Files Used for Stability Analysis

Appendix B: Hardware Data Sheets

Appendix C: First Order Equation Synthesis

Appendix D: PBASIC Controller Code